

SURFACE ROUGHNESS AND CELL REACTION TO HYDROPHOBIC
MATERIALS

A Major Qualifying Project Submitted to the Faculty of
WORCESTER POLYTECHNIC INSTITUTE

In partial fulfillment of the requirements for the
Degree of Bachelor of Science

By

Matthew Horwedel

September 1st, 2019

Approved:

Dr. Christopher Brown, Primary Advisor
Department of Mechanical Engineering, WPI

Dr. Robert Daniello, Co-Advisor
Department of Mechanical Engineering, WPI

This report represents the work of WPI undergraduate students submitted to the faculty as evidence of completion of a degree requirement. WPI routinely publishes these reports on its website without editorial or peer review.

Acknowledgements

The collective knowledge and expertise of individuals are what makes scientific inquiry an exercise in exploring the world in which we live, rather than a legitimization of dogmatic attitudes based upon preconceived notions. The Surface Metrology lab is acknowledged as a place where ideas are the currency and authority entrusted to the scientific process, motivated by understanding the world in which we live. The individuals, both past and present, are also appreciated for their contributions to a lab environment supportive of scientific inquiry and mutual respect. The only “buy-in” to the lab is curiosity, motivation and a willingness to learn.

Matt Gleason is valued for his diverse multidisciplinary knowledge he has brought with him to Surface Metrology. The level of patience and attentive devotion to enriching the author’s understanding and working knowledge of Surface Metrology are a rare find at WPI in those pursuing a PhD; excellent traits for any future professor.

Hudson Gasvoda is thanked for his many hours of very competent instruction using the Sensofar S neox 3D Profiler. Hudson’s maturity and willingness to help are scarce in the current academic climate. As a taxpayer, the author is personally thankful for Sensofar’s generous donation of their S Neox optical 3D profiler to the lab, providing an invaluable opportunity to explore surface metrology research with their elegant 3-in-one confocal, interferometric and Ai focus variation microscope. Thanks to Nathaniel Rutkowski for his contribution of data analysis software and his exceptional kindness in explaining this software, as the author was out of practice.

The author thanks Christopher Brown and Robert Daniello for their guidance, collective experience, kindness and time shared. Professor Brown and Daniello are invaluable assets to WPI who help the institution live up to its highly marketed reputation.

Abstract

The potential to utilize the material properties of wettability of a surface, concerning the hydrophobic and hydrophilic characteristics are significant to cell adhesion on surfaces. The use of wettability properties correlated with geometric surface features is valuable particularly in applications where other factors are not as advantageous. The hydrophobicity of a surface can be affected by chemically active groups, as well as the geometric features at micron scale level. The material property of wettability affected by surface features of geometric characterization is an area of study this report aims to explore through treatment of biocompatible surfaces with various grits of sandpaper and correlations with cell surface adhesion. The adhesion of cells to surfaces is conventionally measured by the classical sense of adhesion with force per unit area holding the cell to the surface. The report aimed to count cell coverage of a surface when compared to other surfaces treated with different sandpaper grits, which would differentiate between adherent and non-adherent surfaces, rather than the adherent strength. The direction aimed to find an optimal scale and multiscale surface measurement parameter to reproducibly control cell adhesion with sand paper for future studies.

Contents

Acknowledgements.....	1
Abstract.....	2
Contents.....	3
List of Figures	4
List of Tables.....	5
1.0 Introduction	6
1.1 Objective.....	6
1.2 Rationale	6
1.3 State-of-the-Art	9
1.3.1 Surface Measurement and Analysis.....	9
1.3.1.1 Topographical Geometric Characterization	9
1.3.1.2 Conventional Characterization of Surface	9
1.3.1.3 Multiscale Analysis	11
1.3.2 Wettability.....	13
1.3.2.1 Optimal Contact Angles	13
1.3.3 Surface Coverage by Cells.....	13
1.3.3.1 Microscopy.....	13
1.4 Approach	14
2.0 Methods	14
2.1 Analytic Techniques	14
2.1.1 Surface Roughness	15
2.1.2 Surface Coverage by Cells	16
2.2 Analysis of Surface to Cell Reaction	17
2.3 Flow Chart.....	18
3.0 Results	18
3.1 Analytic Techniques	18
3.1.1 Surface Roughness	18
3.1.2 Surface Coverage by Cells	23
3.2 Analysis of Surface to Cell Reaction	23
3.2.1 Surface Roughness Correlation: S_a , S_{ku} , and S_{pk} with Grit	25

3.2.2 Relative Area Correlation: Complexity	27
4.0 Discussion.....	32
4.1 Analytic Techniques	32
4.1.1 Surface Roughness	32
4.1.2 Surface Coverage by Cells	33
4.2 Analysis of Surface to Cell Reaction	34
5.0 Conclusion	35
6.0 References.....	36
7.0 Appendices	38
Appendix A	38
Appendix B	38
Appendix C.....	39

List of Figures

Figure 1 Hard steel cylinder for 6 N force(top left), PVC sleeve (top right) and the two assembled (bottom) with sample on the end.	15
Figure 2 The sample treatment device assembled and secured, with the hard steel cylinder in the PVC sleeve, sample attached above the sander also secured with a vice.	16
Figure 3: Plastic petri dish with treated specimens of PTFE, foam polystyrene, and clear polystyrene from left to right. Arranged from top to bottom down each column from left to right, representing the materials, are successive sandpaper grit number treatment specimens. The top of each column in the above orientation, corresponds to a grit number that descends in value going down the column. The farthest left column starts at top with 400 grit then down to 120 grit at the first element of the second column from the left. Two descending cycles of the grit number applied for each material are represented in succession.	17
Figure 4: A flow chart of the experimental process, according to plan.	18
Figure 5 : Relative area to scale graph of clear polystyrene (PS) treated with 120 (Blue), 240(Yellow), 320(Green), and 400 (Red) grit sandpaper.....	19
Figure 6: Relative area to scale graph of foam polystyrene (Opaque PS) treated with 120 (Blue), 240 (Yellow), 320 (Green), and 400 (Red) grit sandpaper.	19
Figure 7 Relative area to scale graph of clear polytetrafluoroethylene (PTFE) treated with 120 (Blue), 240(Yellow), 320(Green), and 400 (Red) grit sandpaper.	20
Figure 8: Relative area to scale graph of clear polystyrene (yellow), polystyrene foam (blue), and polytetrafluoroethylene (green) all treated with 120 grit sandpaper.	21
Figure 9: Relative area to scale graph of clear polystyrene (yellow), polystyrene foam (blue), and polytetrafluoroethylene (green) all treated with 240 grit sandpaper.	22
Figure 10: Relative area to scale graph of clear polystyrene (Yellow), polystyrene foam (Blue), and polytetrafluoroethylene (Green) treated with 320 grit sandpaper.	22

Figure 11: Relative area to scale graph of clear polystyrene (Yellow), polystyrene foam (Blue), and polytetrafluoroethylene (Green) treated with 400 grit sandpaper.	23
Figure 12: Complexity to scale graph of clear polystyrene (PS) treated with 120 (Blue), 240 (Yellow), 320 (Green), and 400 (Red) grit sandpaper.	28
Figure 13: Complexity to scale graph of foam polystyrene (PS Opaque) treated with 120 (Blue), 240 (Yellow), 320 (Green), and 400 (Red) grit sandpaper.	29
Figure 14: Complexity to scale graph of polytetrafluoroethylene (PTFE) treated with 120 (Blue), 240 (Yellow), 320 (Green), and 400 (Red) grit sandpaper.	30
Figure 15: Complexity to scale graph of clear polystyrene (yellow), polystyrene foam (blue), and polytetrafluoroethylene (green) all treated with 120 grit sandpaper.	30
Figure 16: Complexity to scale graph of clear polystyrene (yellow), polystyrene foam (blue), and polytetrafluoroethylene (green) all treated with 240 grit sandpaper.	31
Figure 17: Complexity to scale graph of clear polystyrene (yellow), polystyrene foam (blue), and polytetrafluoroethylene (green) all treated with 320 grit sandpaper.	31
Figure 18: Complexity to scale graph of clear polystyrene (yellow), polystyrene foam (blue), and polytetrafluoroethylene (green) all treated with 400 grit sandpaper.	32
Figure 19: A sample of polystyrene treated surfaces from two specimen of the material with two sandpaper grit number treatments.	39

List of Tables

Table 1: Clear polystyrene S_a , S_{ku} , and S_{pk} values for sandpaper grits 120, 240, 320, and 400.	25
Table 2: Foam polystyrene S_a , S_{ku} , and S_{pk} values for sandpaper grits 120, 240, 320, and 400.	25
Table 3: PTFE S_a , S_{ku} , and S_{pk} values for sandpaper grits 120, 240, 320, and 400.	25
Table 4: S_a , S_{ku} , and S_{pk} values for clear polystyrene (PS clear), foam polystyrene (PS Opaque), and PTFE treated with 120 grit sandpaper.	26
Table 5: S_a , S_{ku} , and S_{pk} values for clear polystyrene (PS clear), foam polystyrene (PS Opaque), and PTFE treated with 240 grit sandpaper.	26
Table 6: S_a , S_{ku} , and S_{pk} values for clear polystyrene (PS clear), foam polystyrene (PS Opaque), and PTFE treated with 320 grit sandpaper.	26
Table 7: S_a , S_{ku} , and S_{pk} values for clear polystyrene (PS clear), foam polystyrene (PS Opaque), and PTFE treated with 400 grit sandpaper.	27

1.0 Introduction

1.1 Objective

The objective of this project is optimization of surface roughness in a repeatable manner as it positively correlates to cell adhesion via hydrophilicity and negatively to superhydrophobicity. The larger scope is to use the correlation to assist in designing a 3D construct of stacked 2D cell laden patterns of adherent cells, where the patterns are formed by controlling the regional surface roughness.

1.2 Rationale

Cellular adhesion to surfaces is significant for many physiological events, including wound healing, blood clotting, immune response and acceptance of implanted biomedical materials. Applications include use of stents, biosensors, most implants, study of drug effects *in vitro*, drug delivery *in vivo* and pathology of many diseases (Bae, W.G., 2016). Cellular surface adhesion is a process that is influenced by many factors both intrinsically and extrinsically in relation to the cell. The proteins involved directly with cell surface adhesion, such as integrins and ligands, the pH of the microenvironment, the morphology of the cell and chemical as well as material properties of the surface are some of the main factors that influence surface adhesion of cells (Ranella, A., 2010).

The potential of geometric characterizations of hydrophobicity could be of use in applications where chemical hydrophobicity presents variables that affect more than what is desired, like cell differentiation stability of cardiac myocytes (Shimizu, 2001)

Cells adhere to surfaces by protein recognition of proteins that are bound to a surface, such as ligands (Britland, S., 1996). The cell senses the protein which adsorbs to the surface and the cytoskeleton reacts to the bonds formed along with the extracellular matrix, which is the scaffolding of the cell's environment. The protein quaternary and tertiary structure in part also determines if hydrophobic/phillic domains are exposed, to promote adhesion, which is in part dictated by the roughness of the fractal like pattern of a protein surface profile. Several environmental cues, like temperature, have been used to control cell adhesion to surfaces to make patterns (Shimizu, T., 2001).

The protein adsorption to the surface is partially dependent on the hydrophobicity, which is in part, correlated with the roughness (Ishizaki, T., 2010). The surface that is already hydrophobic (chemically) can be made superhydrophobic with a certain roughness and geometrical topographic features at an optimal scale (Rosales-Leal, J.I., 2010). Cells favor hydrophilic surfaces for adhesion based upon the wettability alone, which arises from chemical and topographical features (Wang, Y., 2006). Proteins involved in cell adhesion are thermodynamically favored to adhere onto a hydrophobic surface (Wang, Y., 2006). Hydrophobicity of a surface can be conditioned through a process of roughening the surface if it is a chemically hydrophobic surface, to produce a superhydrophobic surface (Nilsson, M.A., 2010). Surfaces that are not hydrophobic by chemistry, can be treated to have a roughness with optimal wettability which can increase cell adhesion (Chang, H.I., 2011). The controllable aspect of a material roughness can be used to make patterns on a surface and therefore, direct cell adhesion into a desired pattern (Bae, W.G., 2015).

The correlation between surface roughness of a hydrophobic material and cell adhesion is valuable because it can be used to condition a surface without additional chemicals to effect cell adhesion (Kim, J., Bae, W.G., 2016). The minimal addition of chemicals is significant when utilizing a living construct to avoid complications that may be

toxic to life, inconvenient for certain time scales and to decouple effects on the studied specimen that may arise from the chemical, aside the influence of the topography itself (Hahn, M.S., 2006).

The translational possibilities of further investigating superhydrophobic surface correlations to roughness are applicable to protein purification optimization as well as potential cancer treatment as it applies to adhesion of metastasized cancer cells (Chen, W., 2016). The roughness parameters applied to the surface and morphology of cells, could also be potentially used as an early diagnostic for breast cancer (Wang, Y., 2016).

The wettability of a surface is relevant to cell adhesion due to the preference of cellular adhesion to hydrophilic surfaces (Chang, H.I., 2011). The relevance of cell adhesion to a surface that is a manufactured construct is applicable to the medical field for tissue interfaces of implantable materials, tissue constructs like tissue engineered blood vessels and diagnostics requiring devices that interact with tissues via direct contact (Shimizu, T., 2001). Indirectly, the subject of hydrophobic surfaces can also lend itself to the pharmaceutical industry for protein purification and drug delivery (Kaczor, A.A., 2012).

1.3 State-of-the-Art

1.3.1 Surface Measurement and Analysis

1.3.1.1 Topographical Geometric Characterization

Scanning profilometry is used to measure surfaces and is a compilation of 2D profiles that can be put together for a 3D profile. Optical microscopy using light is also used to get a 3D profile of surfaces and is limited in its precision by the 200nm limit of light wavelength. Atomic force microscopy (AFM) can also be used to measure a surface stiffness (Lydon, M.J., 1985). The Sensofar 3D optical profiler will be used on the interferometric setting to measure the treated surfaces. The measurements then are analyzed using Mountains Maps software to characterize what the optimal roughness is as it correlates to cell adhesion (Rosales-Leal, J.I., 2010).

1.3.1.2 Conventional Characterization of Surface

The correlation between cellular interaction and surface roughness is applied clinically in implants, such as dental or orthopedic applications, where bone ingrowth and osteoblast activity are involved with the integration of the implant. The topography of an implantable surface is traditionally characterized with surface texture, light reflective properties and with measurement parameters in 2D of R_a , R_t and R_z as well as S_a , S_z , S_q , and S_t in 3D (ASME B46.1), are used for biomedical applications involving isotropic surfaces (Seonwoo, H., 2016). Metal alloy, polymer and naturally derived materials are used for implants where other cell interactions with surface roughness, such as local immune response, can occur (Salhouse, T.N., 1984). Surface measurements of a biocompatible surface can be grouped into two main categories of cross sections of the surface in amplitude measurements and by 3D measurements of the surface with spatial parameters. The calculations used to characterize the materials treated, are S_{pk} , S_a , and S_{ku} . The parameters

used in this application of surface metrology are classified within roughness as being of height and functional parameters. The arithmetic mean height (S_a) and kurtosis (S_{ku}) are height parameters of the surfaces and describe an average of heights as well as the distribution of their sharpness. The kurtosis of a surface, S_{ku} , is the amount of height measurements beyond a statistical norm or average height measured. The presence of a kurtosis value larger than 3.0 suggests a significant height distribution above or below the surface average that can be interpreted as the sharpness of a surface; below a 3.0 would mean a skewed surface, with few high peaks or low valleys. The relevance to cell adhesion this parameter quantifies describes how a surface may interact with a cell and the focal adhesions formed as well as the potential intracellular reactions that such a topographical feature could illicit. (Kim, J., Kim, Y.J., 2015). The mean height, S_a , describes quantitatively the absolute value of the heights measured that deviate from the mean plane, lending itself to describing the roughness a cell may encounter. The S_{pk} , the reduced peak height, measures the height of the peaks and valleys above or below what is called the core roughness or average roughness which uses the peak to valley range of height measurements in its approximation of an average roughness. The S_{pk} indicates heights beyond the average in the positive and negative Z direction, suggesting a potential point of high pressure on a cell or perhaps another potential focal adhesion outside the general trend of motile directionality a cell or group of cells may engage along a surface. The potential for the study of anomalous peaks in surfaces lends itself to understanding the reaction force within a cell to external stimuli and how the organization of cytoskeletal elements respond (Wójciak-Stothard, B.,1996).

Cell adhesion is an important part of implantation acceptance and surface roughness has been shown to be one important variable that effects cellular adhesion to biocompatible surfaces (Kim, J., Kim, Y.J., 2015). The potential to use surface roughness as a selective property to direct cell adhesion spatially is a result of surface roughness correlations. The

application could be useful in creating desired patterns of cells as a basic unit of larger constructs, such as two dimensional membranes or layers as would be found in dermal regeneration for wound healing of skin burn victims and further, three dimensional constructs to replace tissue components of organs or systems such as the connective tissue found in joints (Kim, J., Bae, W.G., 2017). Multiple scales of measured roughness have been shown to be significant in cellular adhesion, with most being in the nano- to micro- scale range (Seonwoo, H., 2016).

Currently, surface roughness itself is not used to create constructs. Optimal scales have been reported in literature, suggesting that it may be a viable and cost-effective method of directed cell adhesion (Kim, J., Kim, Y.J., 2015).

1.3.1.3 Multiscale Analysis

The literature supports, through the characterization of the topology and biomechanical interaction of the cellular reaction, the significance of using a multiscale approach to correlate surface roughness to the cell coverage. The cellular adhesion, by technical use of the word, deploys the use of force per square unit of area to hold the cell to a surface in this instance. However, cell coverage still lends itself to the study of relevant surface measures used to study adhesion, due to the physical nature of cell adhesion focal points on surfaces needed for coverage and additionally that adhesion potential of surfaces themselves can be studied through the discrete bonding model (DBM) (Brown, C.A., 2001). The DBM attempts to describe the potential adhesive strength of a surface to the number of bonds that exist on it and given the relative area of a surface to the projected area, higher relative surface areas of rough substrates suggests a concurrent adhesive strength through bond density.

Cellular adhesion is needed for cell surface coverage as cells must interact with a surface, either directly or through some molecular medium, such as ligands or other proteins which require the availability of chemical bonds. The surface roughness has been shown to in fact correlate with increased cellular adhesion (Lydon, M.J., 1985). Further, chemistry is a collisional process and by proxy, the probability of a chemical reaction increases in proportion to chemical interaction physically through intermolecular collisions.

Surfaces were measured with the Sensofar S Neox and then data filtered before multi scale analysis was used by leveling the surface and removing outliers, which the Mountains Software does quite aggressively when compared to other software, like Sfrax. The upper and lower limits of roughness to scale are demarked on the resulting graphs, however the scale that relates the surface measurement to the cellular reaction, which is most plausible based upon the cellular biology, corresponds to the size of the cells themselves. The cells used, NIH 3T3 cell type, are roughly 15 microns in width with any motile or focal adhesion length being proportional. The scales at which roughness correlates with the sandpaper grit used, will be compared with the cellular coverage at scales within range of the cellular width, as pseudopod length may play an important role in the surface to cell reaction.

SEM is not a measurement device, but images can be used to deduce location and possible sources of artifacts. A direct quantification of the surface characteristics is not possible with SEM. The significance is that cells may react differently to anomalous surface features and it's important to look for the real source of the outliers to direct investigation for any correlations to surface to cell interaction if further investigation is needed.

1.3.2 Wettability

1.3.2.1 Optimal Contact Angles

Contact angle of profiled water droplets is a practical method to gather hydrophobicity measurements, although difficult to maintain precision in measurements as they are subjective to the observer. The literature has established some contact angles of the hydrophilic to superhydrophobic range which correlate to sandpaper grit (Nilsson, 2010). The literature shows that advancing and receding contact angles for 400, 320, 240 and 120 grit sandpaper are $140^\circ / 80^\circ$, $150^\circ / 19^\circ$, $150^\circ / 146^\circ$, $151^\circ / 134^\circ$ respectively. The contact angles were also gathered from PTFE, which is a biocompatible material and one of the materials tested in this paper. The range of grits represents a maximum contact angle obtained, at 320 grit and a low hysteresis value. The 240 grit represents a significant grit size as it had the lowest value for hysteresis. Distinction between groups correlated with angles to grits for this paper was assumed to be more likely than with the choice of these contact angles to grit correlations.

1.3.3 Surface Coverage by Cells

1.3.3.1 Microscopy

The Sensofar S Neox under confocal setting is to be used to observe the surface coverage of each specimen within samples of each material under each treatment of sandpaper grit number. The lens used to visualize the cell coverage was to be the 20x, which would also allow for topographical measurements of the cells themselves for future studies involving a quantification of the morphological deviations between sample groups.

1.4 Approach

The surface characteristics related to the topological features of biocompatible materials are studied using three different surface measurement parameters of S_a , S_{ku} , and S_{pk} in addition to multi scale measure of relative area. The choice related to both the significance to cell adhesion processes and for choosing the right geometry, state of the art, measurement as well as statistical significance. The correlation between the surface measurements and cell coverage over each treated surface was to be made by gathering cell coverage as a percentage of sampled surface the cells adhered to compared to no cell coverage. Optimal scale, treatment and geometric features to repeatably control cell adhesion were to be gleaned from the experiment.

Complexity graphs and relative area graphs and surface measurement parameter tables containing corresponding sand paper treatment grit numbers, were used. Relevant sand paper grit numbers were chosen based upon established literature relating them to contact angles for the type of surfaces treated (Nilsson, 2010).

2.0 Methods

2.1 Analytic Techniques

Using scale sensitive fractal analysis for relative area compared to scale and complexity, the treated surfaces will be analyzed. The S_a , S_{pk} , and S_{ku} will be used as parameters to describe the surface topography in a way that is applicable to cell surface interaction. Filtering of data gathered with leveling and non-measured points with

interpolation curves will be used. The complexity would be used to determine the potentially correlative scales at which features that characterize the surfaces exist and to compare to the scale of the cell size of 15 microns.

2.1.1 Surface Roughness

Microscale measurements of surfaces will be used as the limits of the equipment dictate that no less than 200 micrometers of precision. The scale at which can effect cell adhesion through hydrophobicity is at the micro scale, although some cellular processes can be effected at the nano-scale through topological ques (Ranella, A., 2010).

Area scale and complexity to characterize surfaces and height as well as functional topographical geometric parameters to describe the topography. The surfaces were to be prepared using a repeatable method of applying sandpaper grit to the materials using a known force and orbital sander.

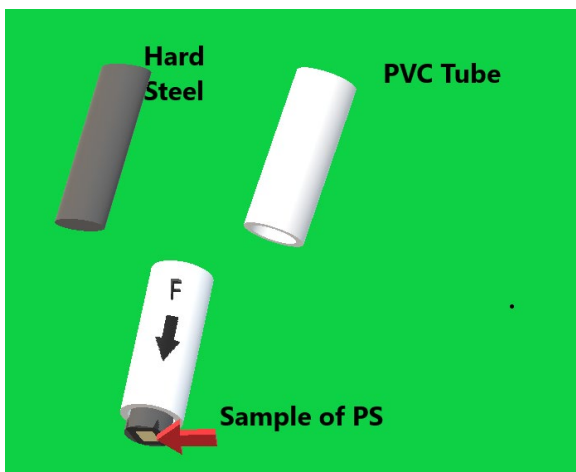


Figure 1 Hard steel cylinder for 6 N force(top left), PVC sleeve (top right) and the two assembled (bottom) with sample on the end.

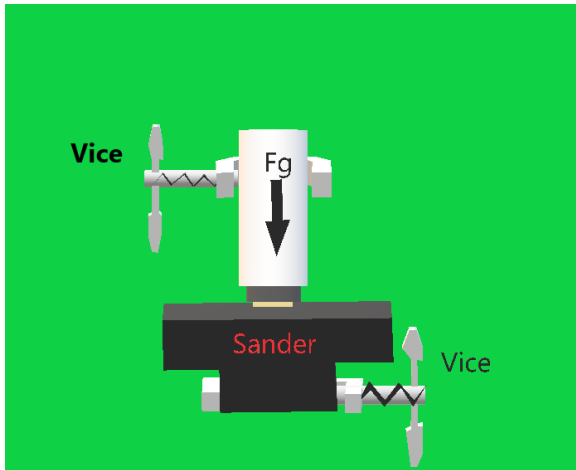


Figure 2 The sample treatment device assembled and secured, with the hard steel cylinder in the PVC sleeve, sample attached above the sander also secured with a vice.

A hard steel metal cylinder was to be used to apply 6.0 N of force to the contact surface of the PS which will be glued stationary to the cylinder. The cylinder will be held in position laterally by a PVC tube, allowing downward movement parallel to gravity and normal to the sample surface.

2.1.2 Surface Coverage by Cells

Cell adhesion will be measured by cell density by light microscope observation to count cells, possibly with Imagej to save time by hand. The coverage of square units of each surface by cells, will be used to compare treatment and materials. The S Neox 3D profiler is chosen for its convenient reflected light mechanism to view the cells on the surface, even without staining. The opaque optical properties of the materials being measured would require more cumbersome culturing methods and less precise microscopy without the use of the S Neox, allowing for a more efficient experimental design as the device is also used for the measurement of the surface topography.

2.2 Analysis of Surface to Cell Reaction

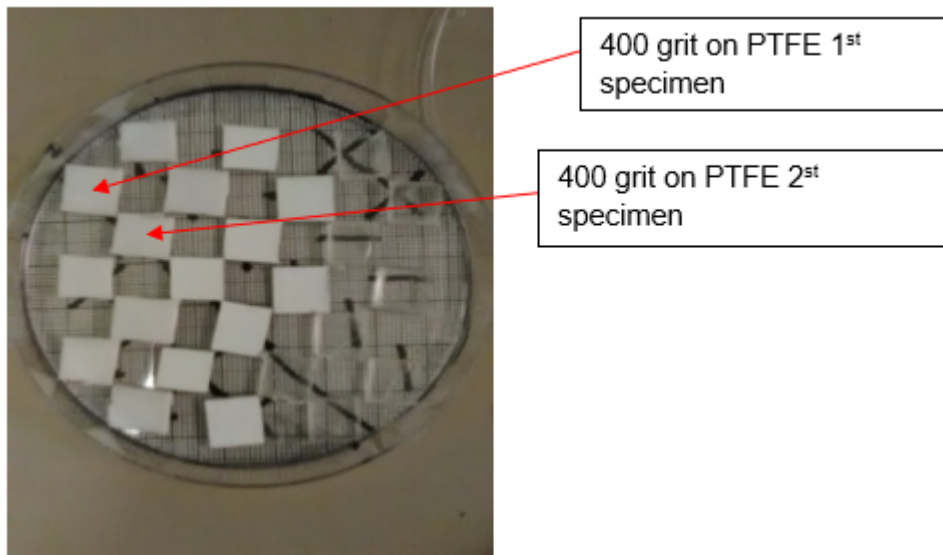


Figure 3: Plastic petri dish with treated specimens of PTFE, foam polystyrene, and clear polystyrene from left to right. Arranged from top to bottom down each column from left to right, representing the materials, are successive sandpaper grit number treatment specimens. The top of each column in the above orientation, corresponds to a grit number that descends in value going down the column. The farthest left column starts at top with 400 grit then down to 120 grit at the first element of the second column from the left. Two descending cycles of the grit number applied for each material are represented in succession.

2.3 Flow Chart

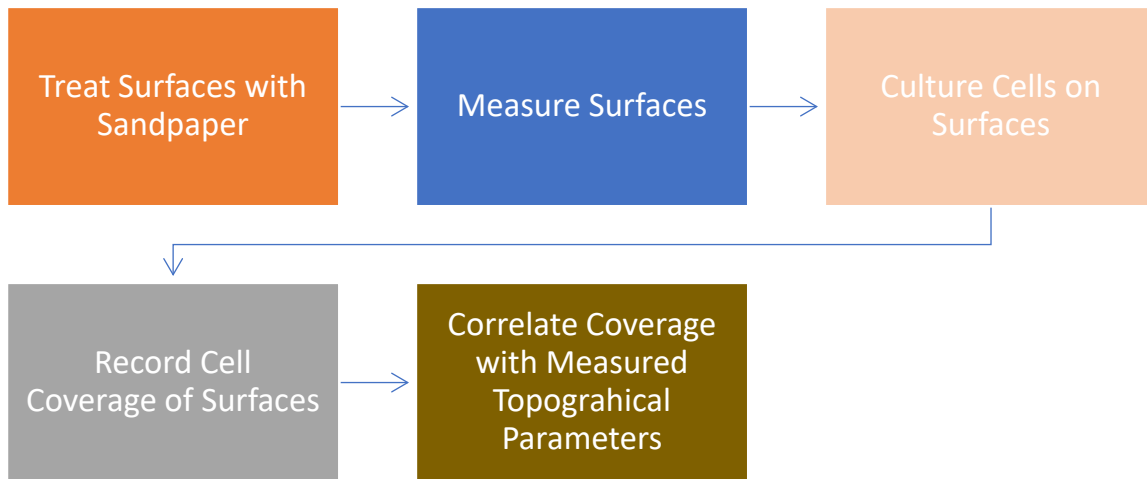


Figure 4: A flow chart of the experimental process, according to plan.

3.0 Results

3.1 Analytic Techniques

3.1.1 Surface Roughness

Relative area plots can be an indicator of surface roughness and in the case of cellular adhesion, potentially yield scales correlated with both grit number and cellular adhesion.

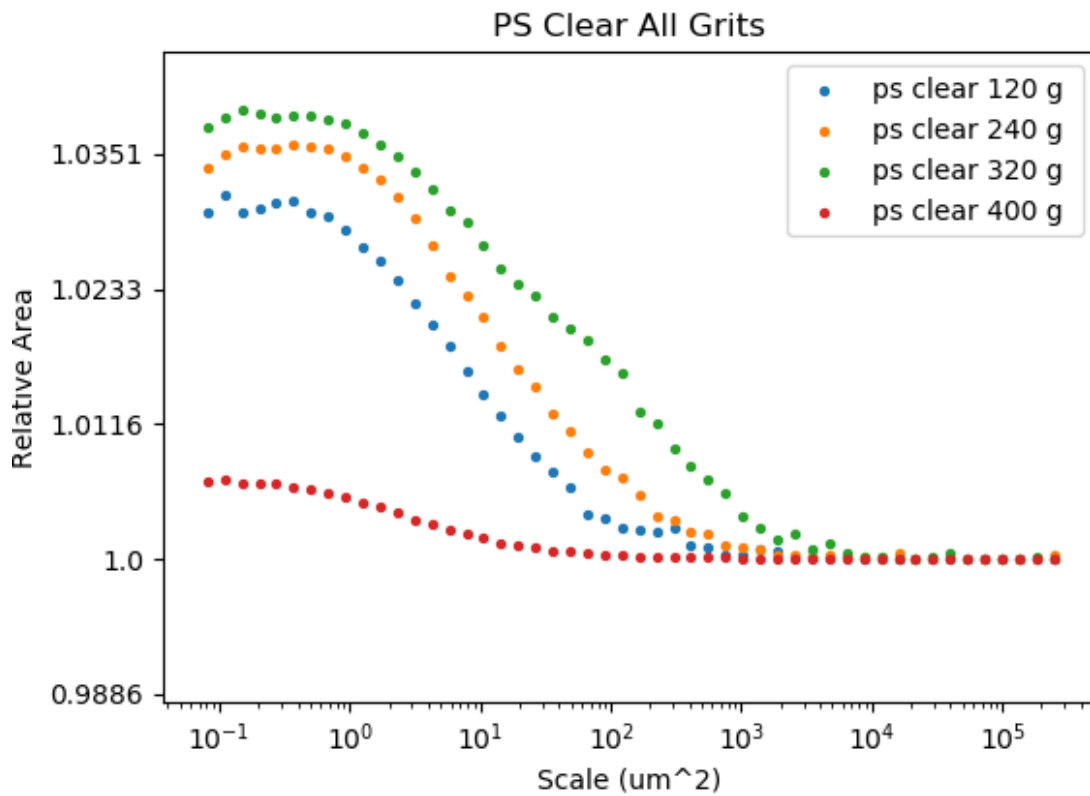


Figure 5 : Relative area to scale graph of clear polystyrene (PS) treated with 120 (Blue), 240 (Yellow), 320 (Green), and 400 (Red) grit sandpaper.

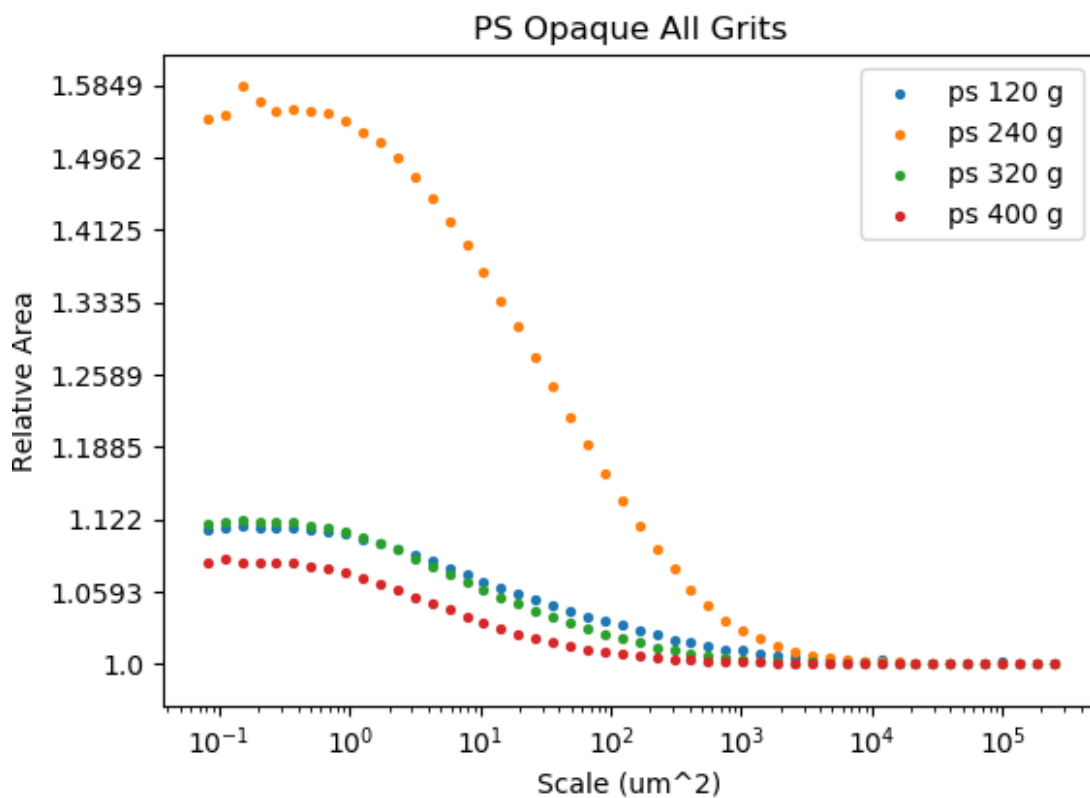


Figure 6 : Relative area to scale graph of foam polystyrene (Opaque PS) treated with 120 (Blue), 240 (Yellow), 320 (Green), and 400 (Red) grit sandpaper.

The 240 Grit curve seems to be an outlier given the fact that the foam PS is one of the softer materials, the larger scale relative area would intuitively have a higher relative area.

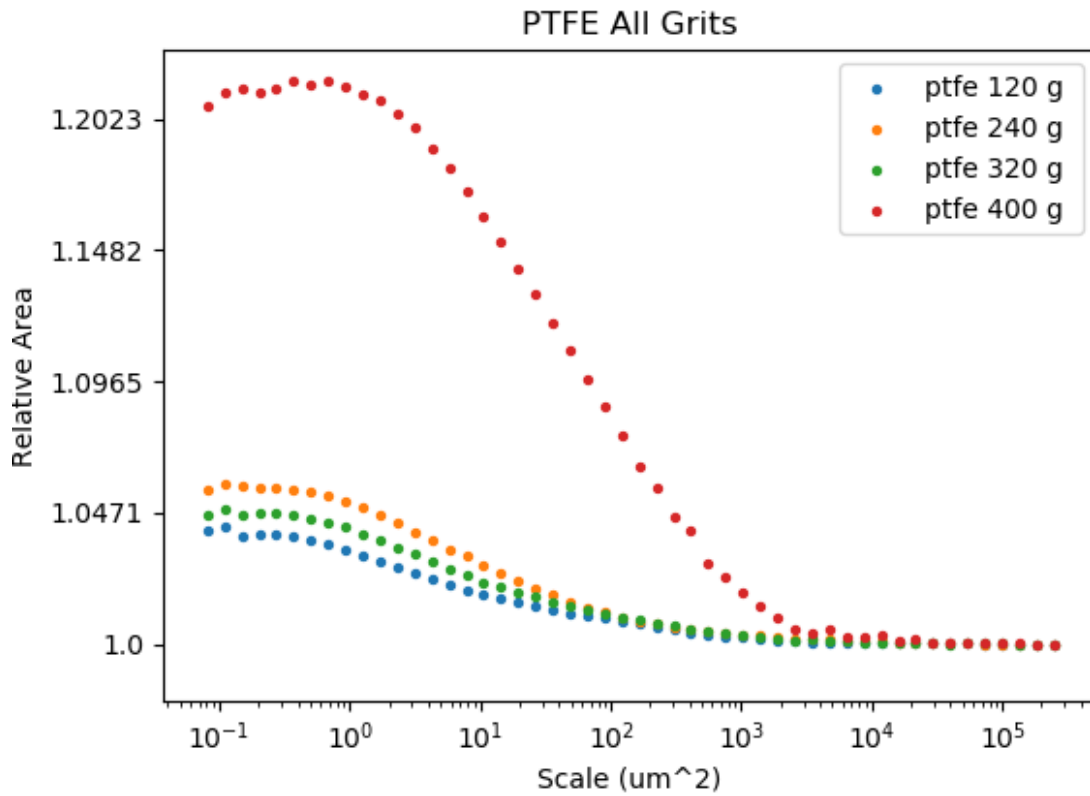


Figure 7 Relative area to scale graph of clear polytetrafluoroethylene (PTFE) treated with 120 (Blue), 240 (Yellow), 320 (Green), and 400 (Red) grit sandpaper.

The 400 Grit curve seems to match intuitively with a higher relative area at lower scales given the finer grit size.

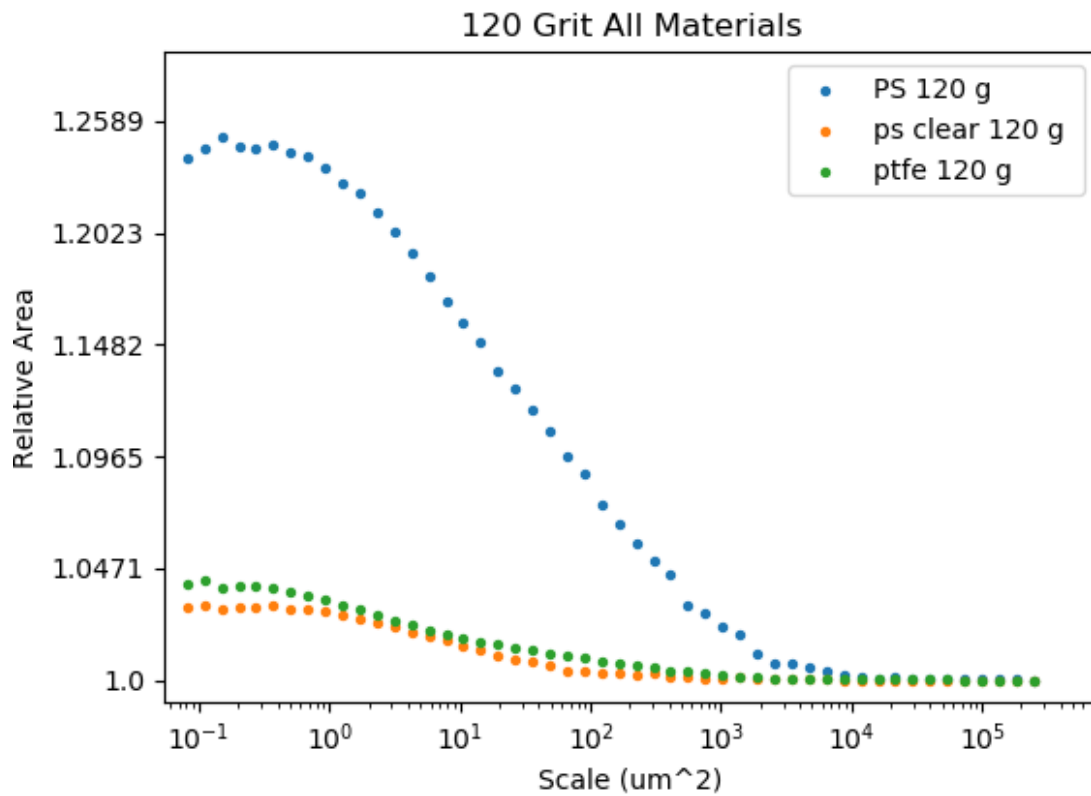


Figure 8: Relative area to scale graph of clear polystyrene (yellow), polystyrene foam (blue), and polytetrafluoroethylene (green) all treated with 120 grit sandpaper.

The foam PS could possibly be an outlier, or a result of inconsistent treatment conditions done by hand.

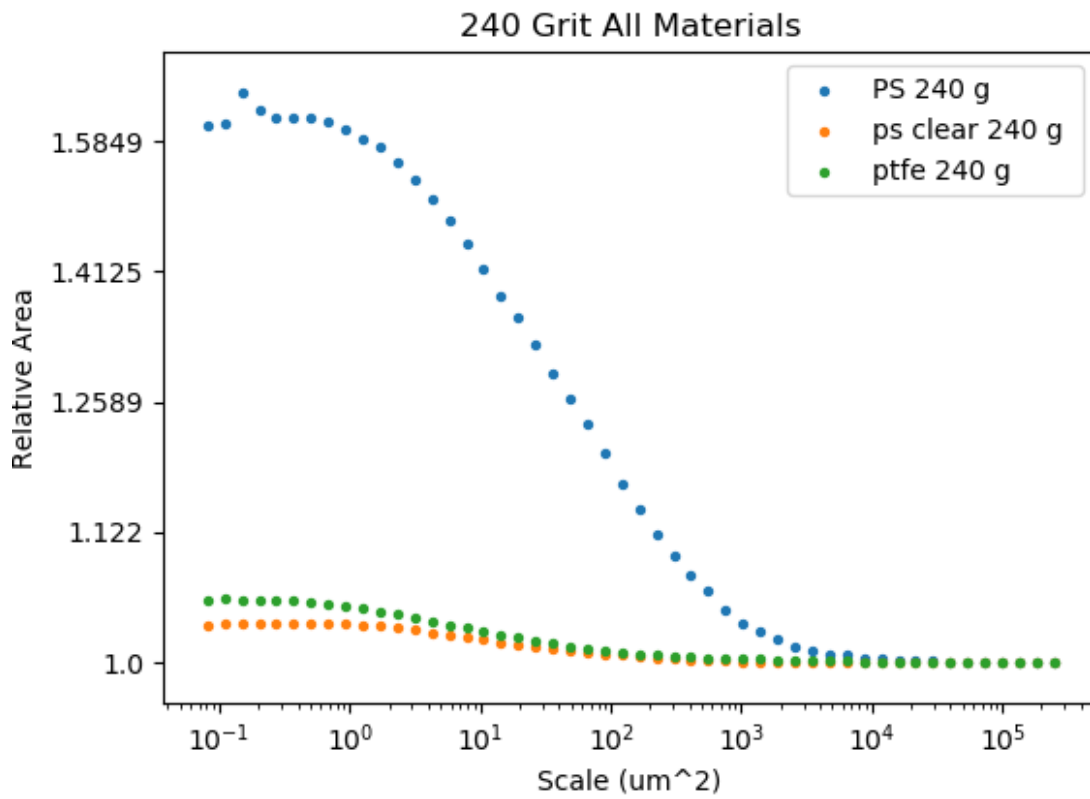


Figure 9: Relative area to scale graph of clear polystyrene (yellow), polystyrene foam (blue), and polytetrafluoroethylene (green) all treated with 240 grit sandpaper.

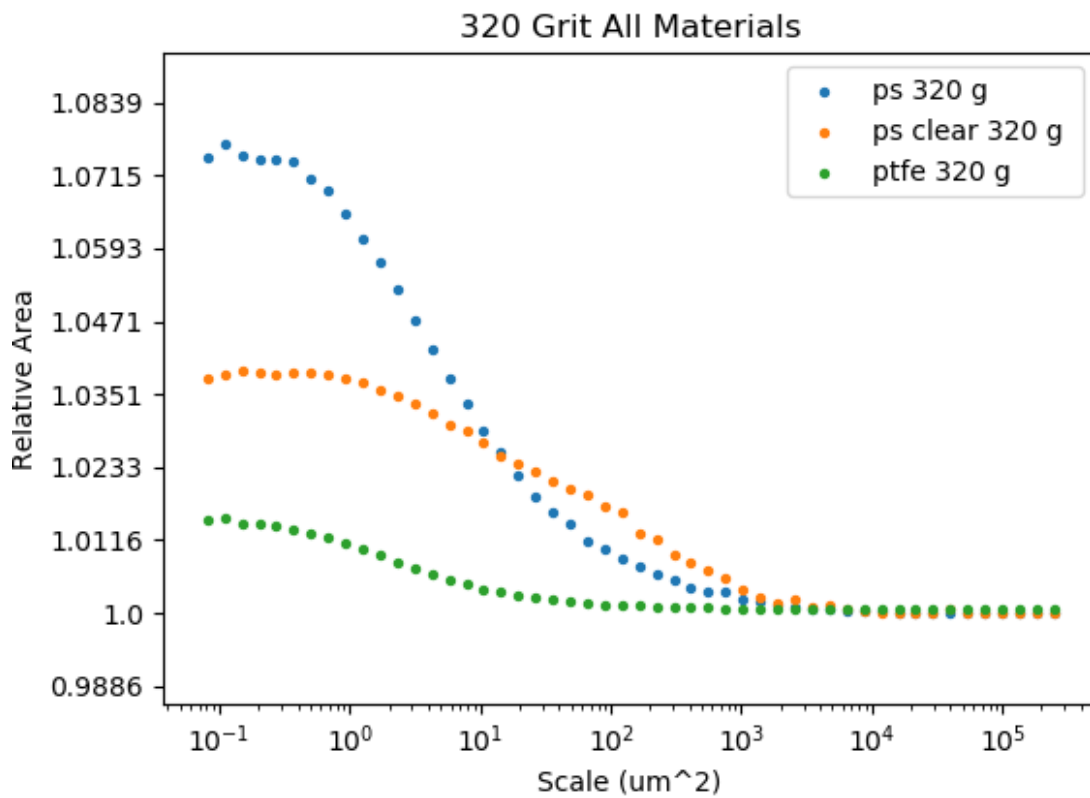


Figure 10: Relative area to scale graph of clear polystyrene (Yellow), polystyrene foam (Blue), and polytetrafluoroethylene (Green) treated with 320 grit sandpaper.

The trend of a lower scale point of deviation of relative areas of each material (Figures 8-10), concurs with the increasing grit number, which should leave a smaller scale impact on relative area.

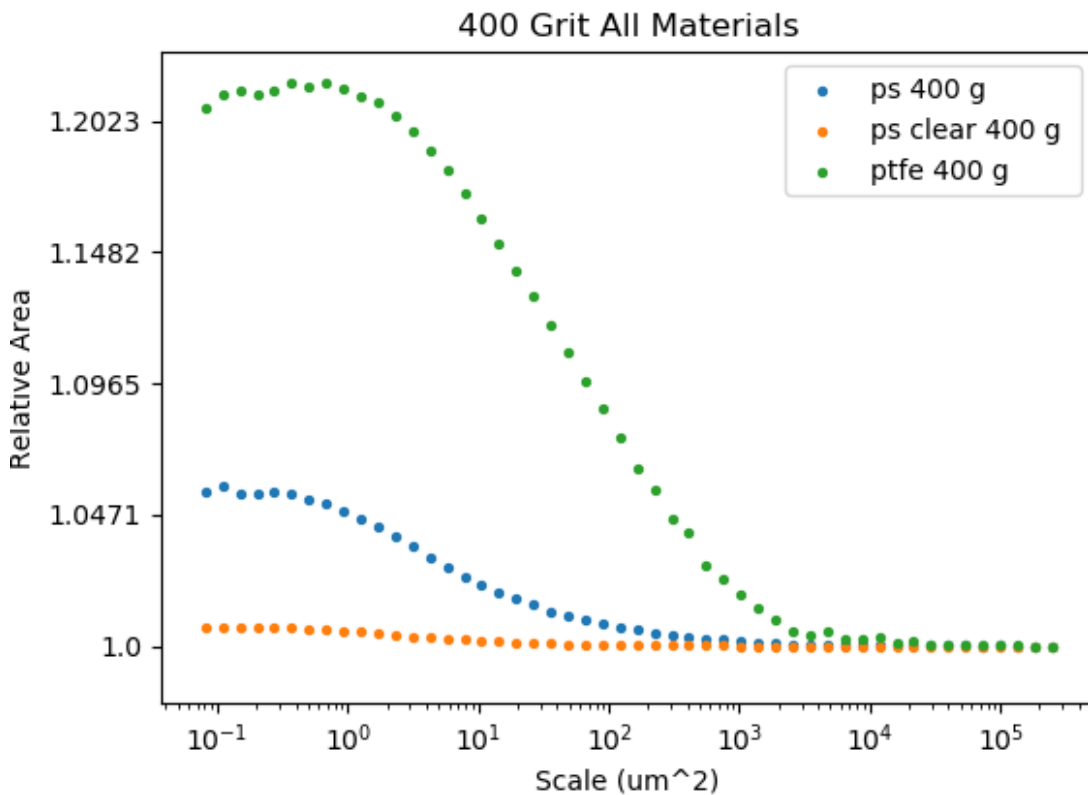


Figure 11: Relative area to scale graph of clear polystyrene (Yellow), polystyrene foam (Blue), and polytetrafluoroethylene (Green) treated with 400 grit sandpaper.

Close large-scale relative area similarity of all materials seems to contradict the trend of the previous graphs where the point of deviation from each other went down as the grit number went up.

3.1.2 Surface Coverage by Cells

3.2 Analysis of Surface to Cell Reaction

No specimen was observed to have cell coverage at all. The cell adhesion was a null result entirely due to a potentially diverse set of environmental factors which may have led to

cytotoxic conditions. Cells were to be counted by percent surface coverage using confocal 3D profiler to view the surface of the opaque samples and measure scale at which cells spread as well as give a quantitative value for morphology.

Green fluorescent protein (GFP) labeled cells were to be obtained which aid in, although not required for, the visualization of cell coverage as well as morphology. The GFP labeled cells would also give insight into the biological component needed to assess the viability of the surface and the microenvironmental conditions with a Live-Dead assay, yielding a percentage of cells that sustained metabolic processes as it the assay indicates cell replication.

Nuclear orientation needed to deduce cell alignment, indicative of topographical influence on cell adhesion in its concurrence with the lay of the features in a specific sample. The overall orientation of micropatterns can be isotropic, however in certain areas of small sample size, there can exist an overall trend of directionality due to the processing of the surface. The characterization of an entire surface of a material and surface treatment will not necessarily be an accurate characterization of the surface. The effect on the cells, however, can be decoupled in their local alignment with the lay and comparing the deviation of alignment with multiple samples from the same material.

3.2.1 Surface Roughness Correlation: S_a , S_{ku} , and S_{pk} with Grit

PS Clear All Grits

Parameter	120 G	240 G	320 G	400 G
S_{ku}	11.7	13.1	14.5	3.66
S_a μm	2.69	2.99	1.21	1.2
S_{pk} μm	7.49	11.8	2.8	1.76

Table 1: Clear polystyrene S_a , S_{ku} , and S_{pk} values for sandpaper grits 120, 240, 320, and 400.

PS Opaque ALL Grits

Parameter	120 G	240 G	320 G	400 G
S_{ku}	204	202	83.9	115
S_a μm	0.272	0.247	0.545	0.12
S_{pk} μm	1.26	0.52	2.77	0.403

Table 2: Foam polystyrene S_a , S_{ku} , and S_{pk} values for sandpaper grits 120, 240, 320, and 400.

PTFE All Grits

Parameter	120 G	240 G	320 G	400 G
S_{ku}	3.36	10.9	28.1	23.8
S_a μm	1.24	1.67	0.97	2.37
S_{pk} μm	1.52	2.58	3.7	5.02

Table 3: PTFE S_a , S_{ku} , and S_{pk} values for sandpaper grits 120, 240, 320, and 400.

Parameters for 120 G All Materials

120 G	S _{ku}	S _a μm	S _{pk} μm
PS Clear	11.7	2.69	7.49
PS Opaque	204	0.272	1.26
PTFE	3.36	1.24	1.52

Table 4: S_a, S_{ku}, and S_{pk} values for clear polystyrene (PS clear), foam polystyrene (PS Opaque), and PTFE treated with 120 grit sandpaper.

Parameters for 240 G All Materials

240 G	S _{ku}	S _a μm	S _{pk} μm
PS Clear	13.1	2.99	11.8
PS Opaque	202	0.247	0.52
PTFE	10.9	1.67	2.58

Table 5: S_a, S_{ku}, and S_{pk} values for clear polystyrene (PS clear), foam polystyrene (PS Opaque), and PTFE treated with 240 grit sandpaper.

Parameters for 320 G All Materials

320 G	S _{ku}	S _a μm	S _{pk} μm
PS Clear	14.5	1.21	2.8
PS Opaque	83.9	0.545	2.77
PTFE	28.1	0.97	3.7

Table 6: S_a, S_{ku}, and S_{pk} values for clear polystyrene (PS clear), foam polystyrene (PS Opaque), and PTFE treated with 320 grit sandpaper.

Parameters for 400 G All Materials

400 G	S _{ku}	S _a μm	S _{pk} μm
PS Clear	3.66	1.2	1.76
PS Opaque	115	0.12	0.403
PTFE	23.8	2.37	5.02

Table 7: S_a, S_{ku}, and S_{pk} values for clear polystyrene (PS clear), foam polystyrene (PS Opaque), and PTFE treated with 400 grit sandpaper.

3.2.2 Relative Area Correlation: Complexity

The complexity plots aim to provide potential insight into a scale where the most change in relative area occurs, suggesting a possible scale within which to investigate significant features. The scales which yield geometric features and relative area concurrent with complexity peak relative area changes, could then be correlated to cell adhesion or grit.

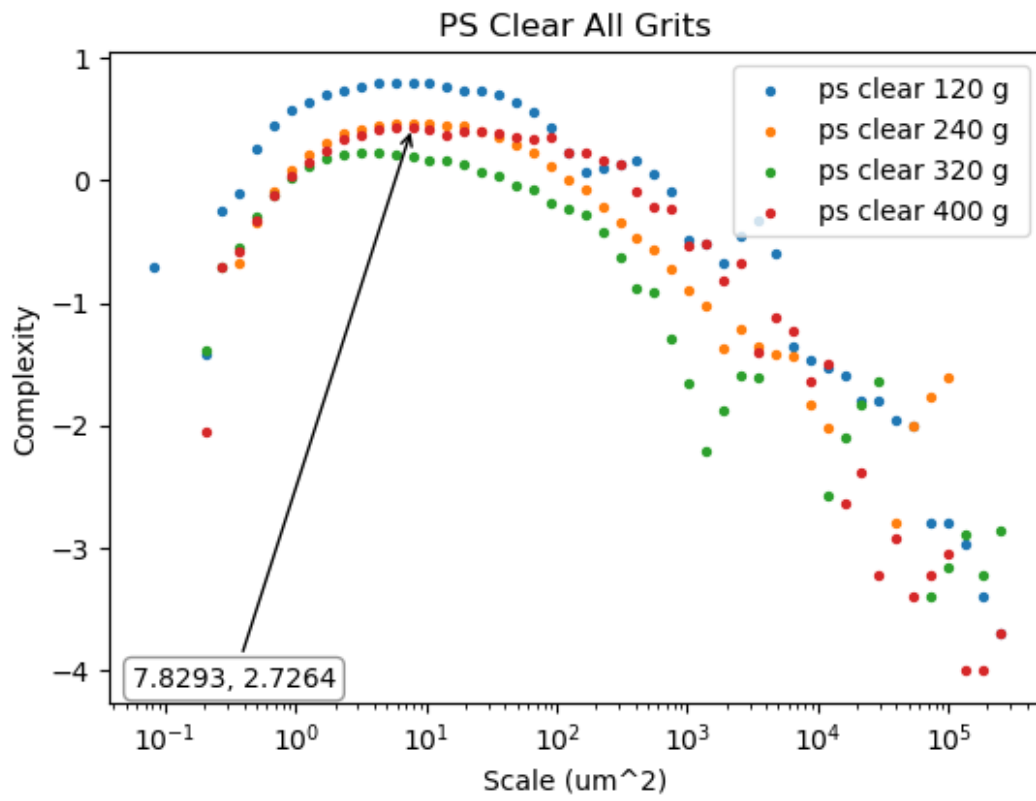


Figure 12: Complexity to scale graph of clear polystyrene (PS) treated with 120 (Blue), 240 (Yellow), 320 (Green), and 400 (Red) grit sandpaper.

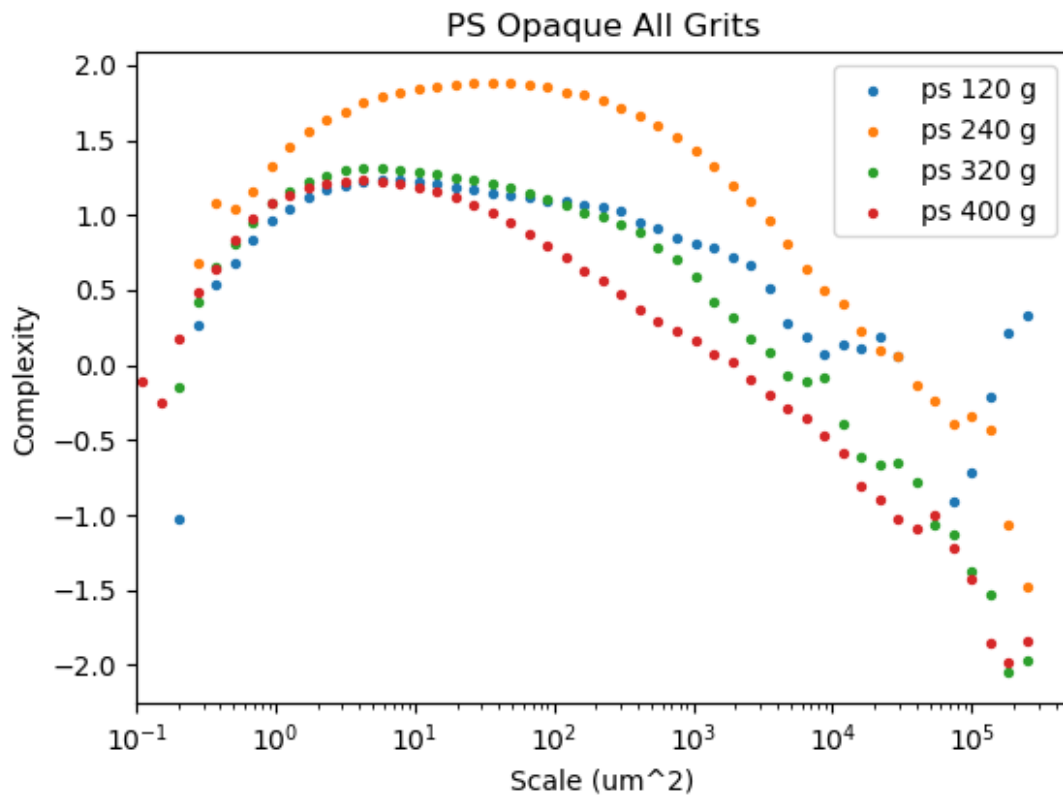


Figure 13: Complexity to scale graph of foam polystyrene (PS Opaque) treated with 120 (Blue), 240 (Yellow), 320 (Green), and 400 (Red) grit sandpaper.

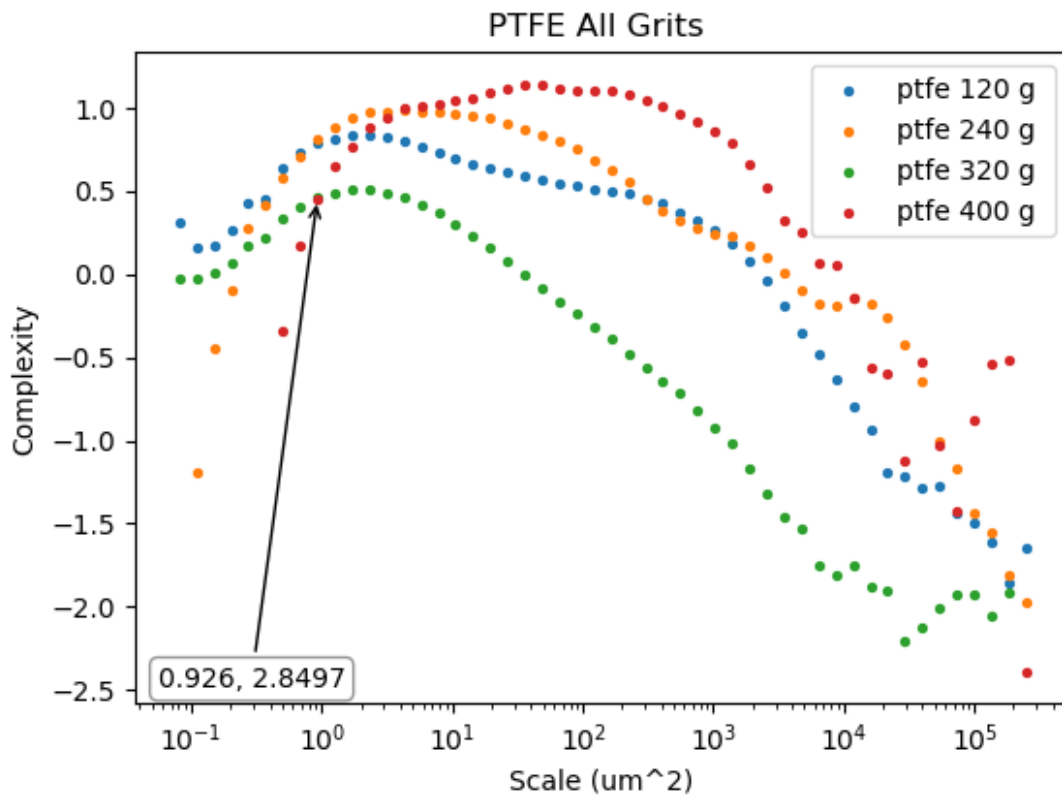


Figure 14: Complexity to scale graph of polytetrafluoroethylene (PTFE) treated with 120 (Blue), 240(Yellow), 320(Green), and 400 (Red) grit sandpaper

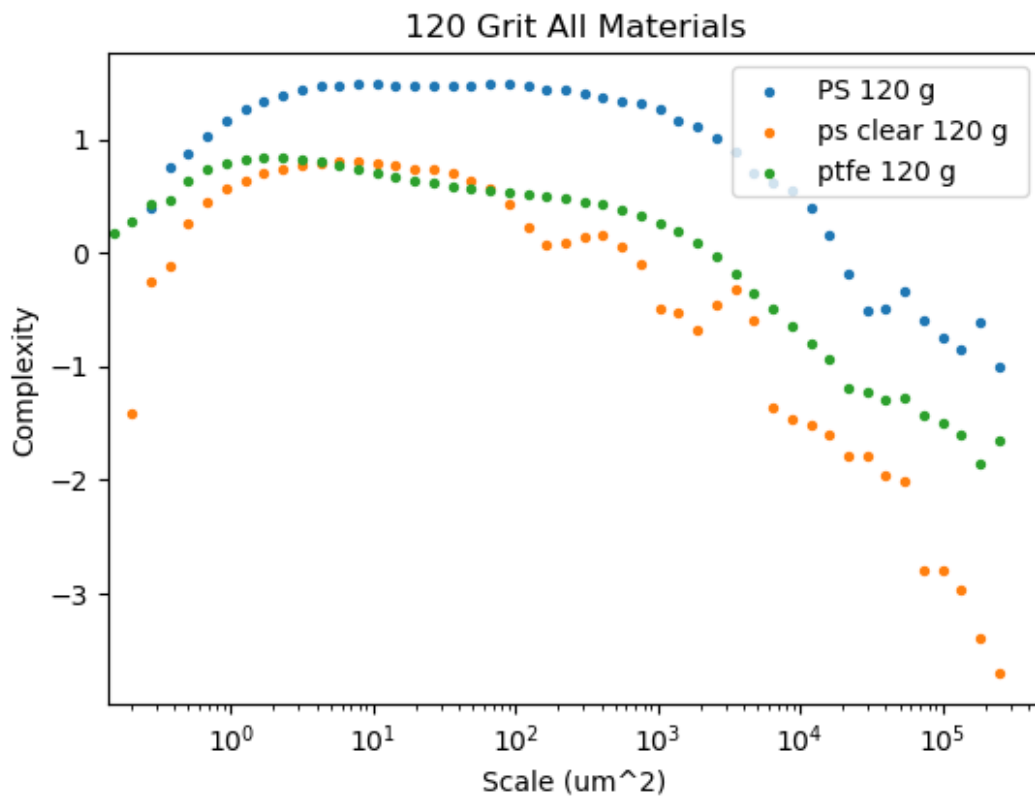


Figure 15: Complexity to scale graph of clear polystyrene (yellow), polystyrene foam (blue), and polytetrafluoroethylene (green) all treated with 120 grit sandpaper.

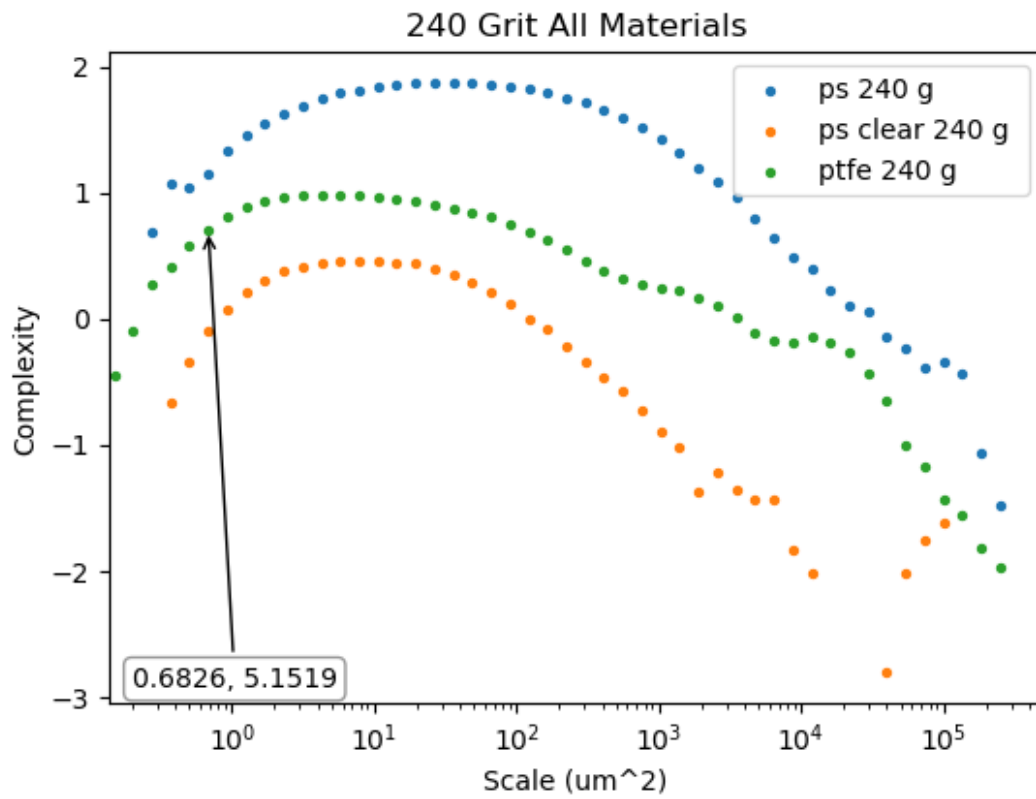


Figure 16: Complexity to scale graph of clear polystyrene (yellow), polystyrene foam (blue), and polytetrafluoroethylene (green) all treated with 240 grit sandpaper.

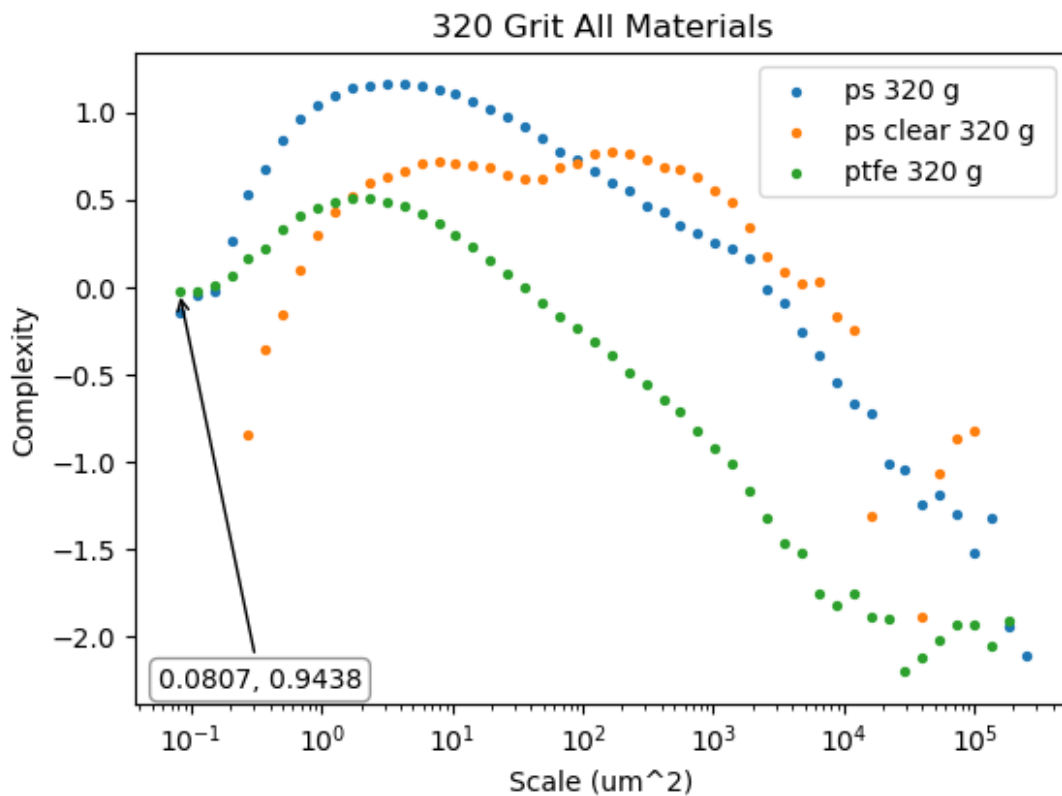


Figure 17: Complexity to scale graph of clear polystyrene (yellow), polystyrene foam (blue), and polytetrafluoroethylene (green) all treated with 320 grit sandpaper.

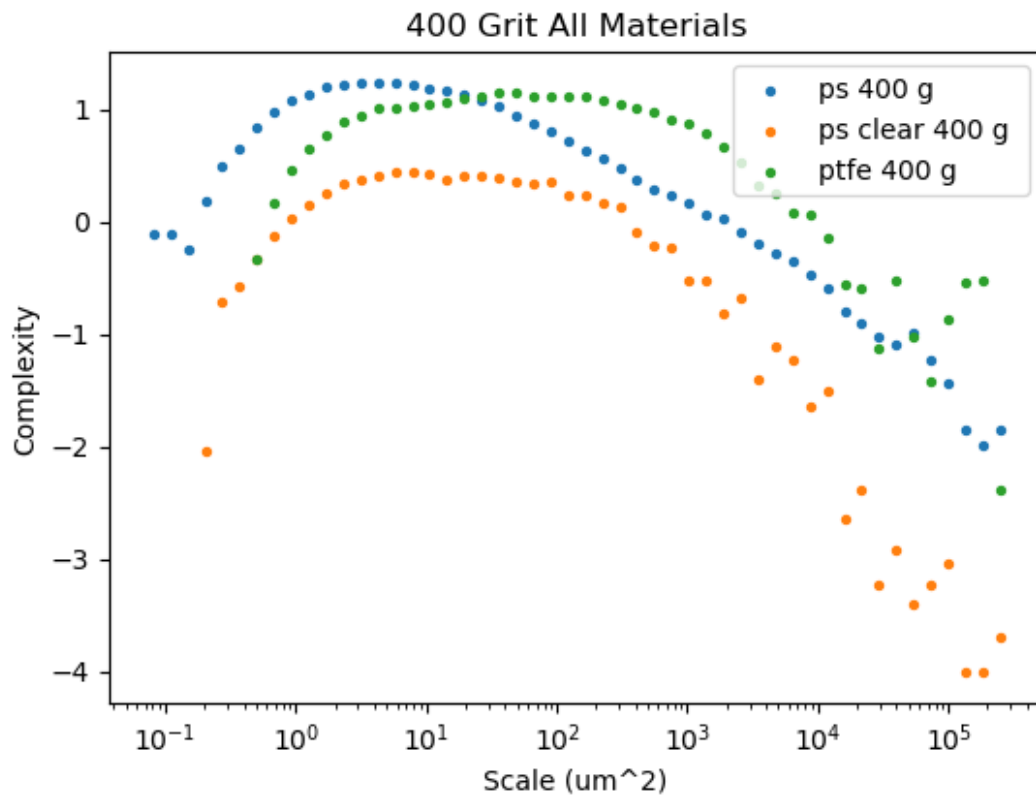


Figure 18: Complexity to scale graph of clear polystyrene (yellow), polystyrene foam (blue), and polytetrafluoroethylene (green) all treated with 400 grit sandpaper.

4.0 Discussion

4.1 Analytic Techniques

4.1.1 Surface Roughness

The filtering of data before the multiscale analysis could have been afterward, as to not filter out potentially significant scales, as they would relate to both significant surface features as well as the cell adhesion correlation. The spatial analysis parameters may also

have lent more insight into the optimal distancing of features spatially as they correlated with cell adhesion and would have required more outlier filtering and non-measured areas to be filled with interpolation curves.

The sample preparation was done by hand, instead of the proposed more repeatable method using a weight and sander to provide a known force with consistent application of sandpaper grit. The variability of pressure, duration and directionality of hand sanding all could have contributed to inconsistent group differentiation between materials and grits. The limits of time and resources contributed to failure to execute the repeatable sample preparation.

The lack of statistically significant samples was an oversight due to time constraints and the number of treatments, four sandpaper grits all together. A higher number of samples per material and treatment would have given a more averaged distribution of values for the roughness at scale than the few sample numbers used for each specimen. Several petri dish culturing sequences would also have helped the repeatability of the process to rule out the effect on cell adhesion by incubation variables, like CO₂ concentration, temperature and heat conductance of the materials influencing the cell viability.

4.1.2 Surface Coverage by Cells

The null result could plausibly have been influenced by factors outside topography, such as the fluid dynamics of the cell culture medium, inhibiting cell adhesion to the surfaces. The fact that the post height of the surfaces was above the cell culture dish bottom, created a high point for the cells to potentially settle onto in order to bond, which would have left the cells settling to the bottom of the culture dish, as it would have been the lowest possible point. The plastic petri dish had warped in the oven, which may have led to cells settling to

the bottom outer circumference of the dish due to the convex deformation curve with the peak in the center of the dish.

The posts placed for the surfaces to study cell adhesion could have been placed in positions below level with the bottom of the dish or perhaps in indentations on a raised surface of PDMS, allowing cells to settle at a low point with the surface samples at the bottom. A better method of allowing cell adhesion would have been to use a known count of cells per mL and then depositing 10 μ L of medium on each surface to sit as a drop while in incubation chamber. The drop would be allowed to let the cells suspended in it to settle to the surface, after which time the rest of the cell culture medium would be gently added as to not wash away the cells, due to hydrostatic or shear forces. After enough time to allow confluency, the surfaces would then be analyzed using SEM imaging and DAPI staining to view nuclear alignment to observe coverage as well as orientation to the topographical features. Additionally, the metabolic state of the cells would be important to note, as the cytotoxicity of the surface effects relate to how viable it would be to potentially make a construct out of the 2D patterned surfaces. The metabolic state of the cells could be observed using Live-Dead assay in order to see whether adherent cells would be viable.

4.2 Analysis of Surface to Cell Reaction

Future study could use the direction this paper offers to expend upon the topographical influence on cells in relation to its connection to wettability of biocompatible surfaces. Surfaces of other material types could also be investigated for their geometric characterization and distinctive variation between groups to see if grit number and materials could be statistically significant contributors to cell adhesion. Also, the cell type could also be investigated, as cell adhesion is a broad subject with many universal factors between cell

types, but there exist more unique conditions for each cell type considering applications of cell adhesion.

SEM imaging could assist in investigating cell reaction by the morphological and cytoskeletal changes. Culturing techniques, such as inverting microscope slides in a cell suspension for culturing, could allow the use of phase contrast microscope to look at cellular surface coverage. Fluoroscopic imaging could also circumvent the need for different culturing conditions if it uses emitted light images, rather than transmitted images that have to pass through an optically transudative material. Finally, use of software, like Imagej, could enable an automated and more repeatable method of quantifying cell coverage by a count of cells as well as alignment in conjunction with staining of the cells.

5.0 Conclusion

The results were inconclusive for the cell coverage correlation to topographical features and multiscale analysis. Although there were null results for cell adhesion to surface roughness correlations and wettability comparisons, the potential for the future research with improved cell culture techniques and the translational potential within protein purification are interesting. Further, a repeatable method for treatment would also be interesting to investigate the effects of on the multiscale analysis and differentiation between groups of material treatments. The results could also be indicative of a very effective way of not allowing cell adhesion to a surface, which could be useful for patterning cell laden surfaces, as a negative print.

6.0 References

1. Anselme, K. and Bigerelle, M., 2005. Topography effects of pure titanium substrates on human osteoblast long-term adhesion. *Acta biomaterialia*, 1(2), pp.211-222.
2. Bae, W.G., Kim, J., Choung, Y.H., Chung, Y., Suh, K.Y., Pang, C., Chung, J.H. and Jeong, H.E., 2015. Bio-inspired configurable multiscale extracellular matrix-like structures for functional alignment and guided orientation of cells. *Biomaterials*, 69, pp.158-164.
3. Bigerelle, M., Anselme, K., Dufresne, E., Hardouin, P. and Iost, A., 2002. An unscaled parameter to measure the order of surfaces: a new surface elaboration to increase cells adhesion. *Biomolecular engineering*, 19(2-6), pp.79-83.
4. Britland, S., Perridge, C., Denyer, M., Morgan, H., Curtis, A. and Wilkinson, C., 1996. Morphogenetic guidance cues can interact synergistically and hierarchically in steering nerve cell growth. *Experimental Biology Online*, 1(2), pp.1-15.
5. Brown, C.A. and Siegmann, S., 2001. Fundamental scales of adhesion and area-scale fractal analysis. *International Journal of Machine Tools and Manufacture*, 41(13-14), pp.1927-1933.
6. Chang, H.I. and Wang, Y., 2011. Cell responses to surface and architecture of tissue engineering scaffolds. In *Regenerative medicine and tissue engineering-cells and biomaterials*.
7. Chen, W., Allen, S.G., Reka, A.K., Qian, W., Han, S., Zhao, J., Bao, L., Keshamouni, V.G., Merajver, S.D. and Fu, J., 2016. Nanoroughened adhesion-based capture of circulating tumor cells with heterogeneous expression and metastatic characteristics. *BMC cancer*, 16(1), p.614.
8. Dowling, D. P. *et al.* (2011) 'Effect of Surface Wettability and Topography on the Adhesion of Osteosarcoma Cells on Plasma-modified Polystyrene', *Journal of Biomaterials Applications*, 26(3), pp. 327–347
9. Hahn, M.S., Taite, L.J., Moon, J.J., Rowland, M.C., Ruffino, K.A. and West, J.L., 2006. Photolithographic patterning of polyethylene glycol hydrogels. *Biomaterials*, 27(12), pp.2519-2524.
10. Ishizaki, T., Saito, N. and Takai, O., 2010. Correlation of cell adhesive behaviors on superhydrophobic, superhydrophilic, and micropatterned superhydrophobic/superhydrophilic surfaces to their surface chemistry. *Langmuir*, 26(11), pp.8147-8154.
11. Kaczor, A.A., Guixà-González, R., Carrió, P., Obiol-Pardo, C., Pastor, M. and Selent, J., 2012. Fractal dimension as a measure of surface roughness of G protein-coupled receptors: implications for structure and function. *Journal of molecular modeling*, 18(9), pp.4465-4475.
12. Kim, J., Bae, W.G., Kim, Y.J., Seonwoo, H., Choung, H.W., Jang, K.J., Park, S., Kim, B.H., Kim, H.N., Choi, K.S. and Kim, M.S., 2017. Directional matrix nanotopography with varied sizes for engineering wound healing. *Advanced healthcare materials*, 6(19), p.1700297.

13. Kim, J., Bae, W.G., Park, S., Kim, Y.J., Jo, I., Park, S., Jeon, N.L., Kwak, W., Cho, S., Park, J. and Kim, H.N., 2016. Engineering structures and functions of mesenchymal stem cells by suspended large-area graphene nanopatterns. *2D Materials*, 3(3), p.035013.
14. Kim, J., Kim, Y.J., Bae, W.G., Jang, K.J., Lim, K.T., Choung, P.H., Choung, Y.H. and Chung, J.H., 2015. Topographical extracellular matrix cues on anticancer drug-induced cytotoxicity in stem cells. *Journal of Biomedical Materials Research Part B: Applied Biomaterials*, 103(6), pp.1320-1327.
15. Lydon, M.J. and Clay, C.S., 1985. Substratum topography and cell traction on sulphuric acid treated bacteriological-grade plastic. *Cell biology international reports*, 9(10), pp.911-921.
16. Nilsson, M.A., Daniello, R.J. and Rothstein, J.P., 2010. A novel and inexpensive technique for creating superhydrophobic surfaces using Teflon and sandpaper. *Journal of Physics D: Applied Physics*, 43(4), p.045301.
17. Phelan, M.C., 2006. Techniques for mammalian cell tissue culture. *Current protocols in molecular biology*, 74(1), pp.A-3F.
18. Ranella, A., Barberoglou, M., Bakogianni, S., Fotakis, C. and Stratakis, E., 2010. Tuning cell adhesion by controlling the roughness and wettability of 3D micro/nano silicon structures. *Acta biomaterialia*, 6(7), pp.2711-2720.
19. Rosales-Leal, J.I., Rodríguez-Valverde, M.A., Mazzaglia, G., Ramón-Torregrosa, P.J., Diaz-Rodriguez, L., Garcia-Martinez, O., Vallecillo-Capilla, M., Ruiz, C. and Cabrerizo-Vilchez, M.A., 2010. Effect of roughness, wettability and morphology of engineered titanium surfaces on osteoblast-like cell adhesion. *Colloids and Surfaces A: Physicochemical and Engineering Aspects*, 365(1-3), pp.222-229.
20. Salthouse, T.N., 1984. Some aspects of macrophage behavior at the implant interface. *Journal of biomedical materials research*, 18(4), pp.395-401.
21. Seonwoo, H., Bae, W.G., Park, S., Kim, H.N., Choi, K.S., Lim, K.T., Hyun, H., Kim, J.W., Kim, J. and Chung, J.H., 2016. Hierarchically micro-and nanopatterned topographical cues for modulation of cellular structure and function. *IEEE transactions on nanobioscience*, 15(8), pp.835-842.
22. Shimizu, T., Yamato, M., Kikuchi, A. and Okano, T., 2001. Two-dimensional manipulation of cardiac myocyte sheets utilizing temperature-responsive culture dishes augments the pulsatile amplitude. *Tissue engineering*, 7(2), pp.141-151.
23. Ventre, M., Natale, C.F., Rianna, C. and Netti, P.A., 2014. Topographic cell instructive patterns to control cell adhesion, polarization and migration. *Journal of the royal society Interface*, 11(100), p.20140687.
24. Wang, Y., Sims, C.E., Marc, P., Bachman, M., Li, G.P. and Allbritton, N.L., 2006. Micropatterning of living cells on a heterogeneously wetted surface. *Langmuir*, 22(19), pp.8257-8262.
25. Wang, Y., Xu, C., Jiang, N., Zheng, L., Zeng, J., Qiu, C., Yang, H. and Xie, S., 2016. Quantitative analysis of the cell-surface roughness and viscoelasticity for breast cancer cells discrimination using atomic force microscopy. *Scanning*, 38(6), pp.558-563.
26. Wójciak-Stothard, B., Curtis, A., Monaghan, W., Macdonald, K. and Wilkinson, C., 1996. Guidance and activation of murine macrophages by nanometric scale topography. *Experimental cell research*, 223(2), pp.426-435.

27. Xu, L.C. and Siedlecki, C.A., 2007. Effects of surface wettability and contact time on protein adhesion to biomaterial surfaces. *Biomaterials*, 28(22), pp.3273-3283.
28. Yoshida, S., Sato, K. and Takeuchi, S., 2013. Sequential micro-assembly of three-dimensional biological microstructures from two dimensional cell-laden micro-plates. *Procedia CIRP*, 5, pp.196-200.

7.0 Appendices

Appendix A

Cell medium protocol

Complete DMEM Dulbecco's modified Eagle medium, high-glucose formulation (e.g., Invitrogen), containing: 5%, 10%, or 20% (v/v) FBS (optional; see recipe) 1% (v/v) nonessential amino acids 2 mM L-glutamine (see recipe) 100 U/ml penicillin 100 µg/ml streptomycin sulfate Filter sterilize and store ≤1 month at 4°C. (Phelan, 2006)

Appendix B

Equations

$$S_{ku} = \frac{1}{S_q^4} \left[\frac{1}{A} \int \int_A Z^4(x, y) dx dy \right]$$

Kurtosis

$$S_a = \frac{1}{A} \int \int_A |Z(x, y)| dx dy$$

Arithmetical mean height

Appendix C

Mountains Measurements

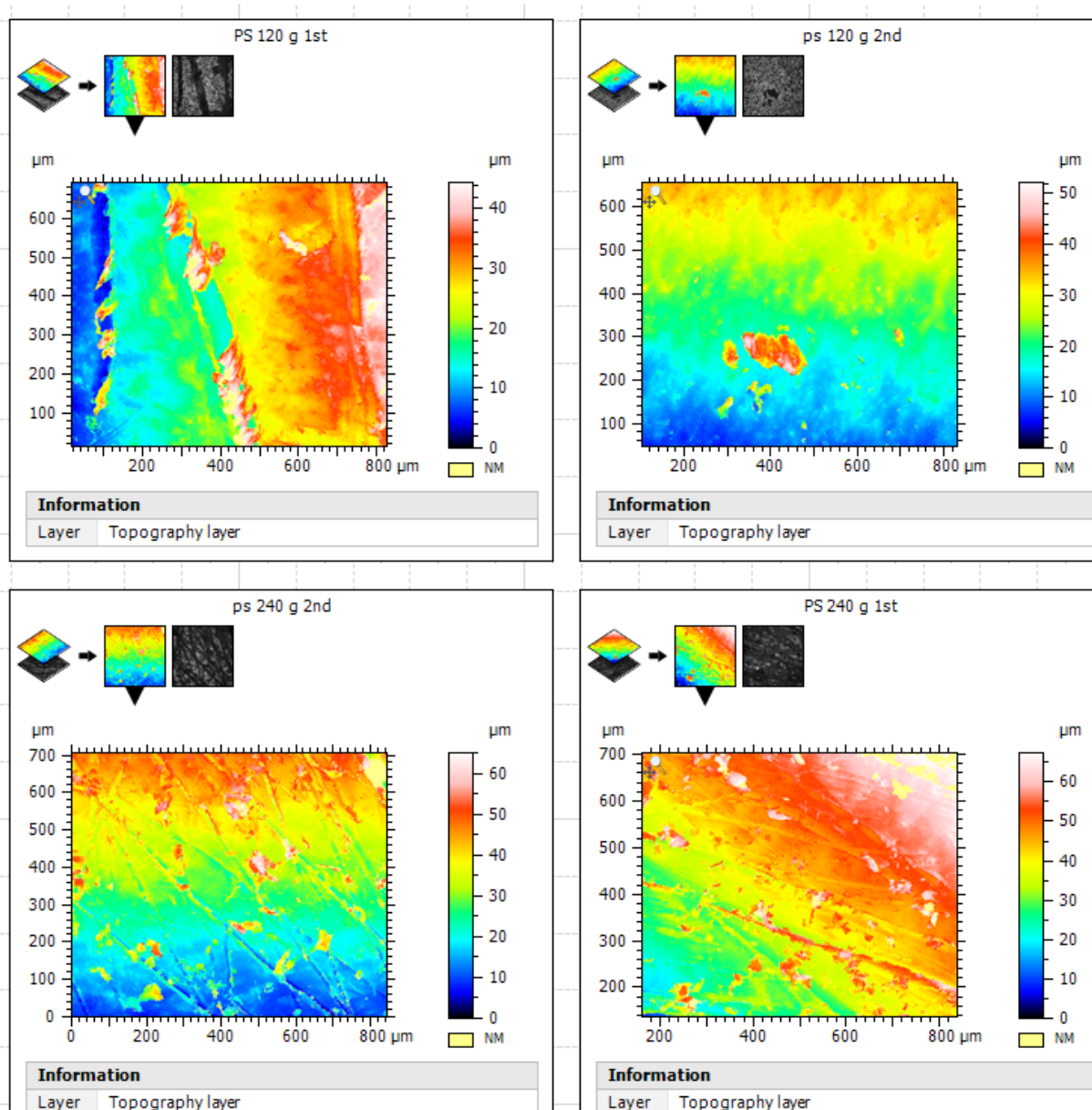


Figure 19: A sample of polystyrene treated surfaces from two specimen of the material with two sandpaper grit number treatments.

